POAC'25
St. John's, Newfoundland and Labrador, Canada

Proceedings of the 28th International Conference on Port and Ocean Engineering under Arctic Conditions
Jul 13-17, 2025
St. John's, Newfoundland and Labrador
Canada

An investigation of the relationship between statistical descriptions of ice conditions extracted from ice profiling sonar data versus sea ice charts

Alka Dash[1], Ian D. Turnbull[1,2], Rocky S. Taylor[1]
[1] Memorial University of Newfoundland (MUN), St. John's, Canada
[2] C-CORE, St. John's, Canada

ABSTRACT

Sea ice monitoring and detection is essential in high latitude regions to support safe maritime activities, navigation, and resource exploration. Understanding key sea ice characteristics—such as concentration, type, floe size, and thickness—is critical for these operations. This study uses Upward Looking Sonar (ULS) measurements collected from three oceanographic moorings—NENS1, NENS2, and NENS3—deployed on the Northeast Newfoundland Shelf. The data, gathered between April 2015 and June 2016 by ASL Environmental Sciences, captures sea ice conditions along the Labrador Current, near the Grand Banks, and Flemish Pass/Orphan Basin.

ULS instruments measure ice draft with high temporal resolution about 1-2 seconds which is converted to ice thickness using the isostatic equilibrium equation. However, ULS data provides only localized measurements meaning they do not provide 2-D spatial coverage. To address this, ice chart data—offering daily ice concentration, floe size, and ice type over broader regions—is integrated with the ULS dataset. To enhance the spatial resolution of ULS data, Inverse Distance Weighting (IDW) interpolation is applied, while linear interpolation improves the temporal resolution of ice chart data. This combined dataset offers a more enhanced spatio-temporal view of sea ice dynamics, capturing how ice conditions evolve as it drifts southwards from NENS1 (51° 50.1491' N) to NENS3 (48° 59.4284' N).

KEY WORDS: Sea ice, Upward looking Sonar (ULS) data, Ice chart, interpolation, Northeast Newfoundland Shelf

INTRODUCTION

The Northeast Newfoundland Shelf is a dynamic marine environment where sea ice pose significant challenges to offshore operations, including navigation, oil and gas exploration, and fisheries. Seasonal ice, transported southward by the Labrador Current, influences oceanographic conditions and necessitates effective monitoring to ensure maritime safety and environmental sustainability. Understanding ice characteristics—such as thickness, concentration, and drift—is crucial for mitigating ice hazards and optimizing operational planning.

To address these challenges, ASL Environmental Sciences conducted an R&D program from April 2015 to June 2016, deploying three oceanographic moorings (NENS1, NENS2, and NENS3) on the Northeast Newfoundland Shelf (Figure 1). These moorings were equipped with Upward Looking Sonar (ULS) to measure ice draft and Acoustic Doppler Current Profilers (ADCPs) to track ice drift velocities, enabling high-resolution sea ice observations.

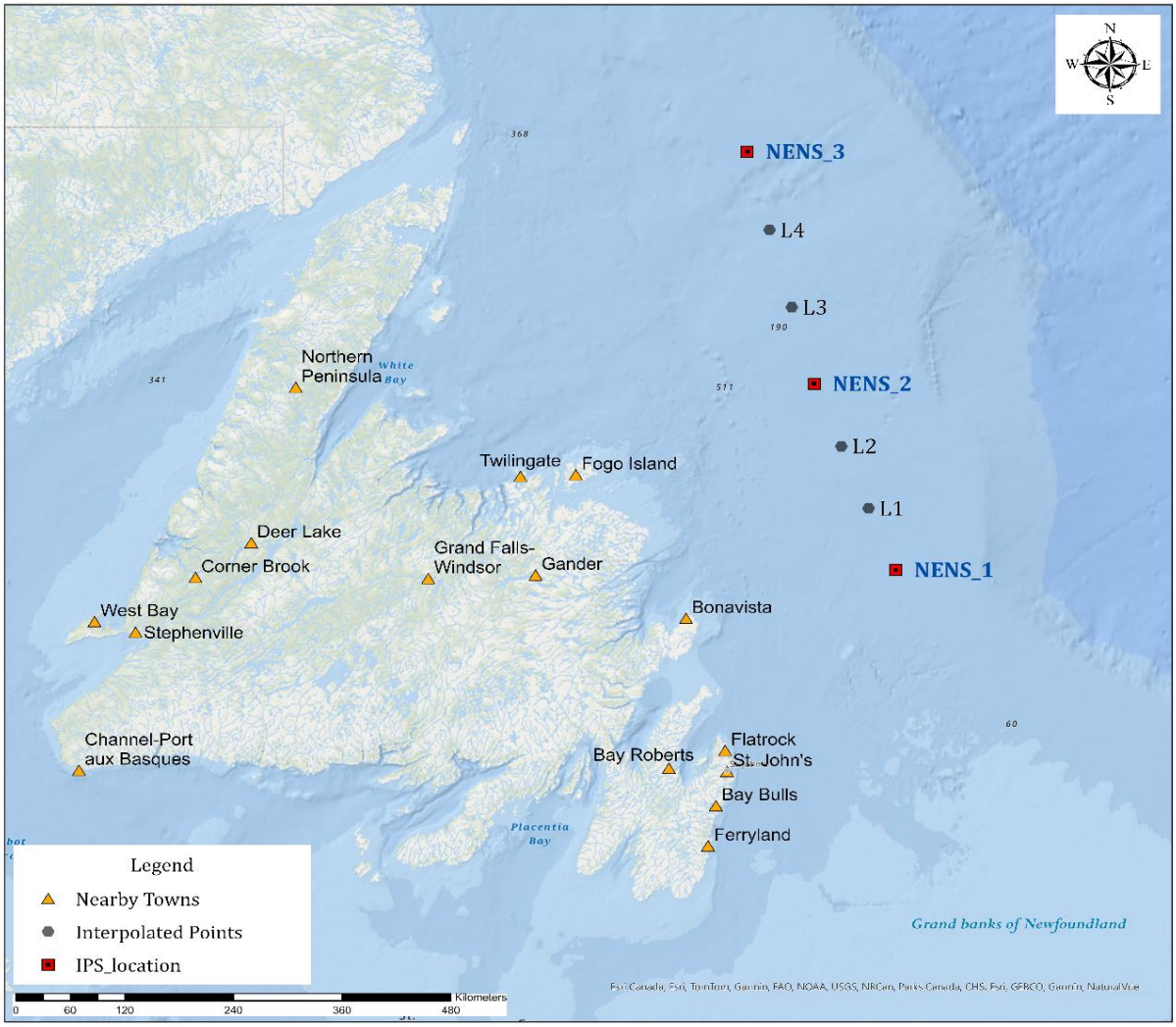

Figure 1: Study area map showing IPS mooring locations (NENS1, NENS2, NENS3), interpolated points (L1, L2, L3, L4), and nearby towns along the Northeast Newfoundland Coast.

Previous studies in the region have explored different aspects of ice conditions. Mudge et al. (2016) used ULS-derived ice draft measurements to estimate floe size distribution, comparing results with satellite imagery and CIS ice charts. They found that ULS effectively detects

smaller floes below satellite resolution, but their study did not assess ice thickness or concentration. Yulmetov et al. (2022) examined pack ice conditions and their impact on offshore structures, integrating CIS ice charts, ULS, and satellite imagery. Their findings emphasized the importance of multi-source data integration for improving ice characterization and offshore design accuracy.

This study takes a detailed approach to analyzing ice thickness and concentration by directly comparing IPS-derived data with CIS chart estimates. It uniquely combines both datasets to overcome their limitations, providing a more accurate depiction of ice conditions. Given the spatial coverage of ULS measurements, which are hundreds of kilometers far from each other, pseudo-data were generated at locations where direct observations were not available using interpolation techniques, allowing for a more detailed comparison with CIS ice charts. Similarly, temporal interpolation was applied to the CIS charts to better align them with ULS data and enable a more refined time-based comparison. This approach aimed to explore the consistency between the two datasets and provide a foundation for future research.

DATABASE OVERVIEW

This study utilizes a specific type of ULS known as Ice Profiling Sonar (IPS) data collected from three moored locations—NENS1, NENS2, and NENS3—on the Northeast Newfoundland Shelf between April 2015 and June 2016. The dataset provides a continuous record of ice draft, sampled every 1 to 2 seconds, allowing for high-resolution analysis of ice keel features, draft variability, and ice thickness distribution. By integrating this dataset with Acoustic Doppler Current Profiler (ADCP) measurements of ice velocity, the IPS-derived ice draft time series can be converted into a spatial series by calculating cumulative ice path lengths. Due to irregular ice drift, a double-weighted double-quadratic interpolation is applied, followed by resampling at 0.10 m and block-averaging to 1.0 m for detailed spatial analysis. The three mooring sites offer broad coverage, with distances of ~145 km between NENS 1 and 2, ~180 km between NENS 2 and 3, and ~340 km between NENS 1 and 3, limiting detailed ice condition assessment.

To get an overview of ice conditions, Ice charts are published by Canadian Ice Service (CIS) daily and weekly covering most of the Atlantic and Arctic waters. These charts, based on satellite data, ship reports, and aerial observations, provide insights into ice concentration (in tenths), ice type or stage of development, and floe size. The ice conditions are represented using the egg code format, where the stage of development gives an indication of ice thickness across all locations. Although the CIS charts offer broad spatial coverage, their temporal resolution is lower, as they are updated only once every 24 hours. By combining IPS data with CIS charts, this study improves the understanding of ice dynamics and variability on the Northeast Newfoundland Shelf.

The study focuses on a 10-day period from March 12 to March 22, 2016, due to the availability of continuous IPS data at NENS2 and NENS3. While data from NENS1 is irregular, it remains relevant and is not excluded from the study. This timeframe represents a critical phase in the ice season, capturing peak ice presence in the region.

METHODOLOGY

This study integrates Ice Profiling Sonar (IPS) data with Canadian Ice Service (CIS) sea ice charts to analyze sea ice thickness and concentration distributions on the Northeast Newfoundland Shelf. The methodology consists of multiple steps, including ice thickness estimation, sea ice concentration analysis, spatial and temporal interpolation, and dataset validation.

Ice Thickness Estimation

The first step involved converting ice draft measurements from IPS to ice thickness using the isostatic equilibrium equation

$$h_i = \frac{(\rho_w \times D) - (\rho_s \times h_s)}{\rho_i} \quad (1)$$

Where h_i = ice thickness [m], D = ice draft [m] measured by the IPS, ρ_w= seawater density [kg/m³], ρ_s = Snow density [kg/m³], h_s = Snow depth [m], ρ_i= Sea ice density [kg/m³]

Since no significant snow cover was present during the selected time frame (March 12–March 22, 2016), a snow-free assumption was applied, setting $h_s = 0$. This assumption was verified using the C3S Arctic Regional Reanalysis (CARRA) dataset. The values for the other parameters in the equation were sourced from various literature. Seawater density (ρ_w) was assumed to be 1025 kg/m³, with an uncertainty of 0.5%, based on Alexandrov et al. (2010) and King et al. (2020). Sea ice density (ρ_i) varied between first-year ice (FYI) and multi-year ice (MYI). For FYI, a density of 916 kg/m³ was used, while for MYI, a density of 882 kg/m³ was considered, with an uncertainty of 30–35%, based on Timco and Frederking (1996), Pustogvar and Kulyakhtin (2016), and Warren et al. (1999).

The derived ice thickness values (h_i) provided high temporal resolution but were spatially limited to the IPS mooring locations. To address this limitation, daily digitized sea ice charts from CIS were incorporated. The ice stage of development from these charts (SA, SB, SC) was converted into thickness estimates using a weighted average approach, considering all three stages of development at each location. Integration of both datasets creates a more comprehensive ice thickness representation, compensating for the limitations of each data source.

Sea Ice Concentration Analysis

To assess sea ice concentration from both IPS and CIS datasets, a systematic classification approach was applied. CIS ice charts provide partial ice concentration for different ice types, categorized as C_A, C_B, and C_C. To align with this classification, IPS-derived ice thickness data was used to calculate ice concentration through weighted average approach within the same thickness categories specified in CIS charts. The concentration was determined using the formula:

$$C_{p,k} = \left(\frac{N_{p.k}}{T_k}\right) \times 100 \quad (2)$$

$C_{p,k}$ = partial concentration for ice type p corresponding to the k_{th} time interval (corresponding to 18:00 UTC on day k to 18:00 UTC on day k+1). $N_{p,k}$ = the number of data points in thickness category p from the IPS record for the k_{th} time interval. T_k = is the total number of points in IPS dataset for the k_{th} time interval. The computed IPS ice concentration values were then compared with the corresponding estimates from CIS charts to assess consistency and identify potential discrepancies in ice classification between the datasets.

Spatial Interpolation and Dataset Validation

To improve spatial coverage, the three study locations (NENS1, NENS2, and NENS3) were connected in a straight-line configuration, and intermediate points (L1, L2, L3 & L4) were considered for further analysis (Figure 1). This approach allowed for the assessment of the consistency between IPS-derived thickness and CIS-based thickness estimates.

Since the IPS data correspond to fixed, discrete mooring locations, the Inverse Distance Weighted (IDW) interpolation method was chosen to estimate ice thickness at intermediate locations along the study transect. These interpolated values were then compared with CIS chart thickness ranges to evaluate spatial consistency.

Temporal Interpolation and Pseudo-Data Generation

Given that CIS ice charts are updated only once every 24 hours, their temporal resolution is much lower than that of the IPS dataset. To bridge this gap, linear interpolation was used to generate pseudo-data points for every 2-hour interval between consecutive CIS thickness values. This generated dataset was then compared with IPS-derived ice thickness measurements, which were already available at a 2-hour frequency. This comparison helped assess how representative the thickness range from CIS charts are when compared to point-based thickness estimates from IPS data.

RESULTS AND DISCUSSION

The analysis of ice thickness and concentration variations was conducted using IPS data and daily ice charts. The daily average IPS values were computed for a 24-hour period from 18:00 on one day to 18:00 the next day, ensuring direct comparability with CIS charts, which are published daily at 18:00 hours (Figure 2).

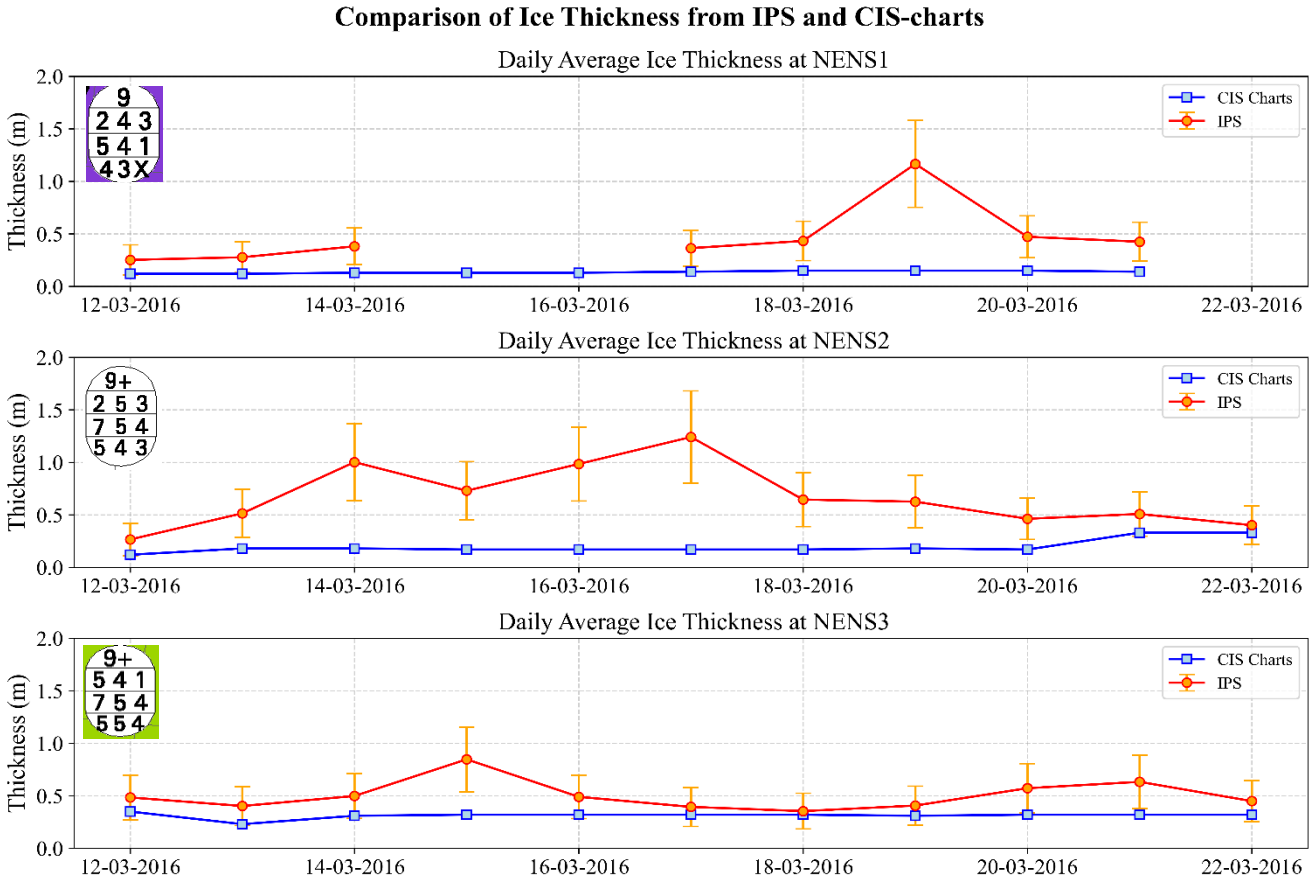

Figure 2: Comparison of daily average ice thickness from IPS with error bars and CIS Charts at NENS1, NENS2, and NENS3 from March 12 to March 22, 2016 (egg codes for 12-03-2016 for validation)

The IPS data revealed significant variability in ice thickness over time, with noticeable peaks likely due to the drift of level ice into the region from areas where thermally grown ice exceeds

1 meter in thickness. This is supported by the high concentration values indicated in the corresponding egg code. The egg code provided for a day (March 12, 2016) helps visually compare different ice environments. In contrast, the CIS data exhibited a much more uniform distribution, lacking the fluctuations observed in the IPS measurements.

A s ice charts are released every 24 hours, generating pseudo-data at two-hour intervals allows for a more detailed comparison with IPS measurements, which provide a finer thickness profile. The comparison between two-hour averaged IPS data and interpolated ice chart estimates is presented in Figure 3. The results again show noticeable differences between the datasets, with IPS capturing the drift of level ice and small ice floes moving in and out of the sonar's view, while CIS values remain relatively steady. At NENS1 (Figure 3-top), the dataset was quite limited, leading to missing data points that made direct comparison difficult. At NENS2 (Figure 3-middle) and NENS3 (Figure 3-bottom), there is a clear rise and dip in IPS thickness estimates, clearly indicating the incoming and outgoing of thin and thick level ice as well as ice floes in the region. A more accurate interpretation of these ice features could be achieved by integrating metocean conditions, which is beyond the scope of this paper.

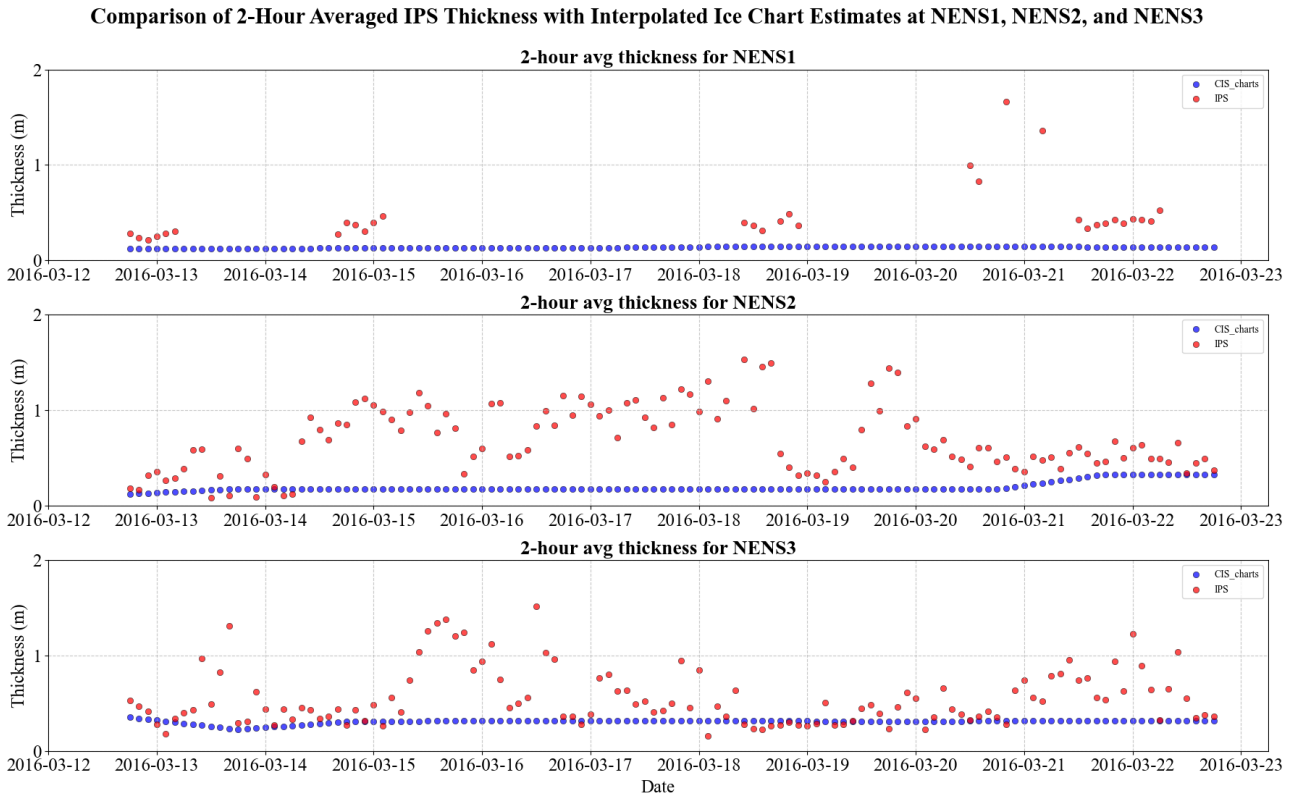

Figure 3: Comparison of 2- hour average ice thickness from IPS and interpolated CIS charts for each mooring location from March 12 to March 22,2016

As mentioned earlier, since the IPS instruments are placed several hundred kilometers apart, interpolation techniques were applied to estimate ice thickness at additional locations (L1, L2, L3, L4). The data at these new locations represent pseudo-data, enabling enhanced comparison of IPS thickness values with the published ice chart data (Figure 4). The results again show considerable differences between the two datasets, with IPS effectively capturing the movement of level ice and ice floes in and out of the sonar view, while ice charts continue to show a more uniform transect of thickness values, missing localized ice movements in the region.

The comparison of ice concentration estimates from IPS data and CIS ice charts reveals notable discrepancies across different mooring locations. At NENS1 (Figure 5), CIS charts report higher ice concentrations in the 10–15 cm category, while IPS data indicate peak concentrations in the 30–70 cm range but with lower overall values. At NENS2 (Figure 6), CIS charts show a peak concentration in the 15–30 cm thickness category, whereas IPS peaks in the 30–70 cm range with lower concentration values. At NENS3 (Figure 7), both datasets exhibit peak concentrations in the 15–30 cm range, demonstrating better agreement, although CIS concentrations remain higher across all categories. This suggests that ice charts capture widespread thin ice concentration, whereas IPS detects thicker ice features passing over the mooring site. These variations can also be primarily taking the midpoint of each thickness range from the ice charts was used as a representative value. This approach may be conservative, potentially underestimating actual thickness if thicker ice dominated within those ranges.

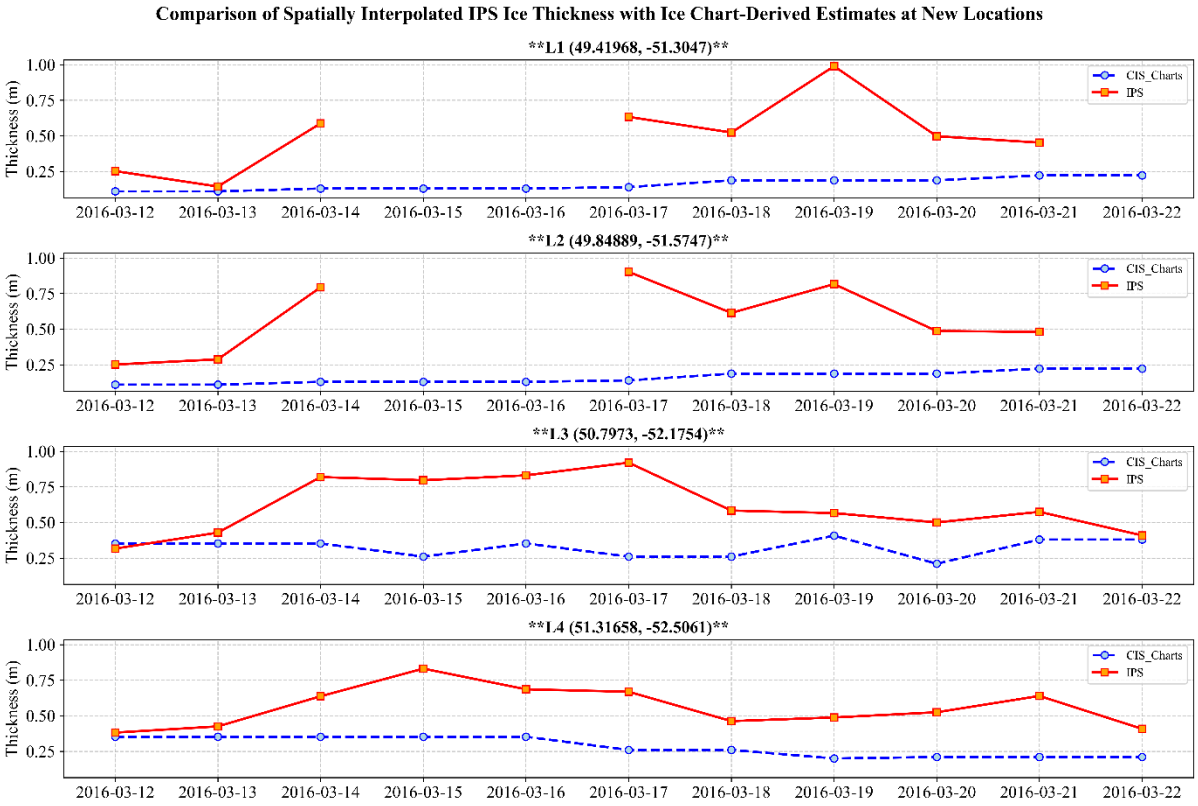

Figure 4: Comparison of interpolated IPS-derived ice thickness (red line) and CIS chart-derived estimates (blue line) for four newly interpolated locations, L1, L2, L3 & L4.

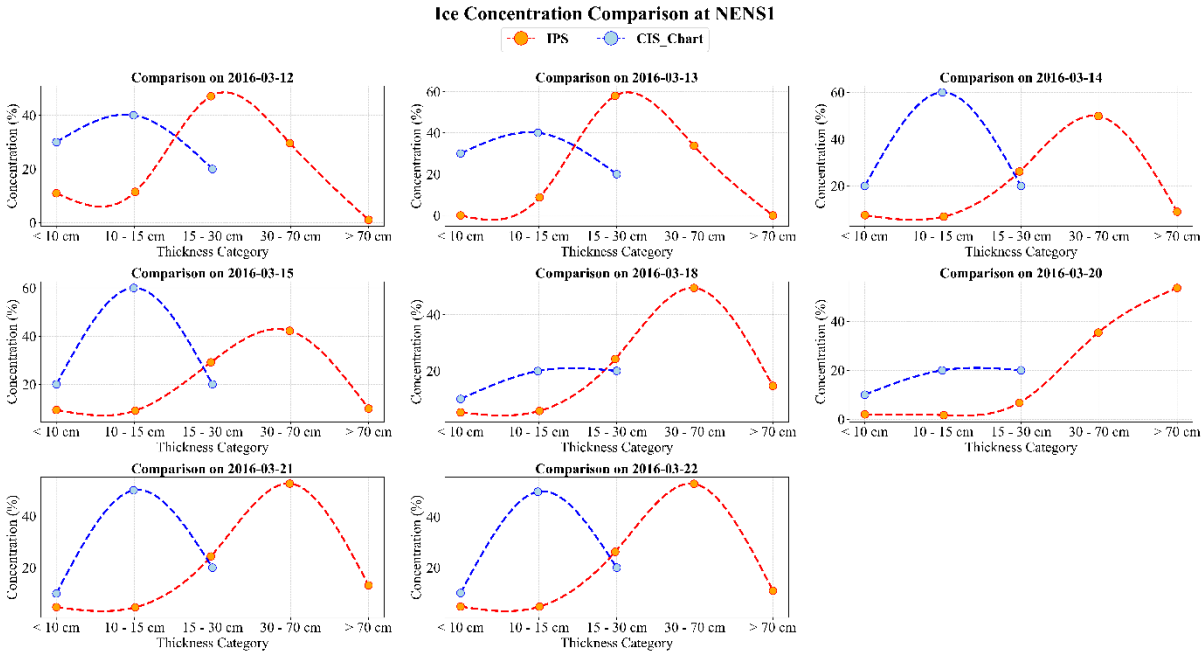

Figure 5: Comparison of Ice Concentration from IPS (yellow, green dashed line) and CIS-estimated (red, blue dashed line) at NENS1 (March 12–22, 2016). Missing dates are due to data unavailability.

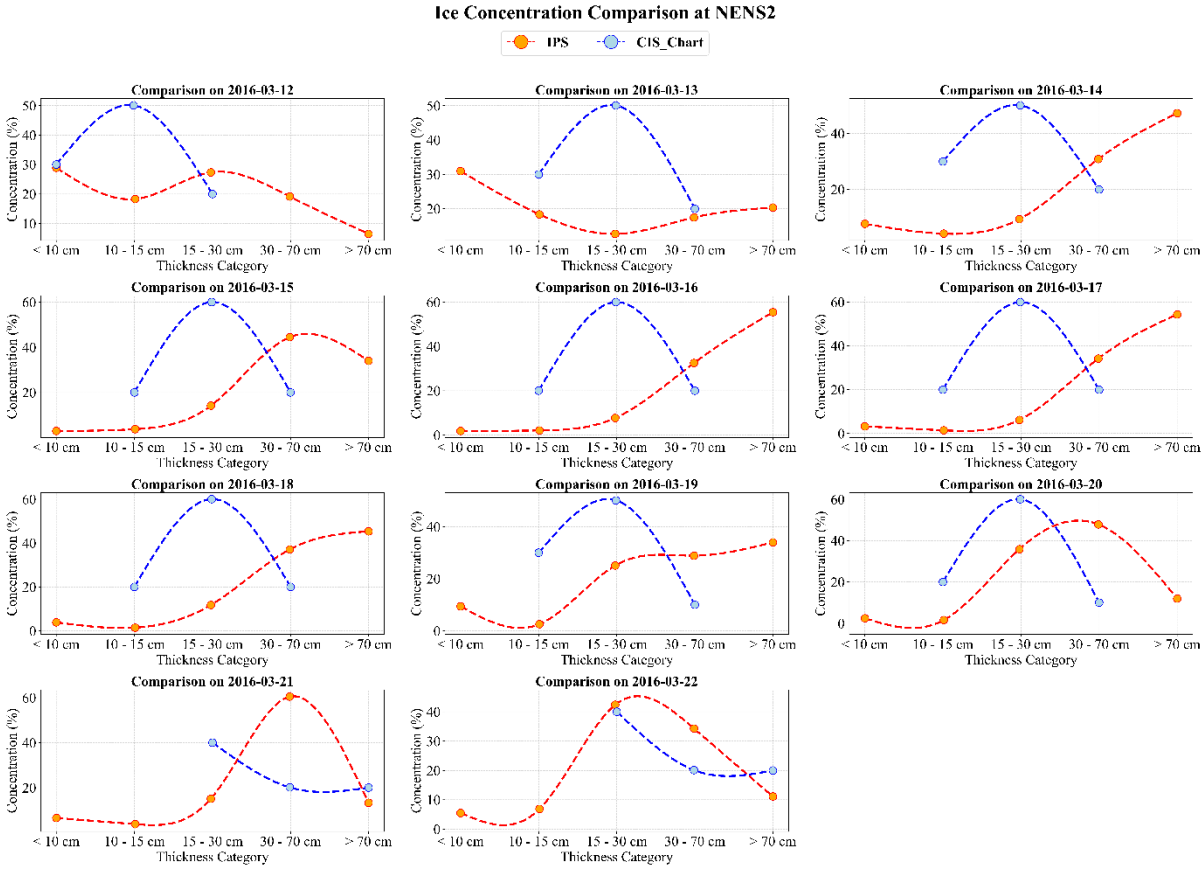

Figure 6: Comparison of Ice Concentration from IPS (yellow, green dashed line) and CIS-estimated (red, blue dashed line) at NENS2 (March 12–22, 2016).

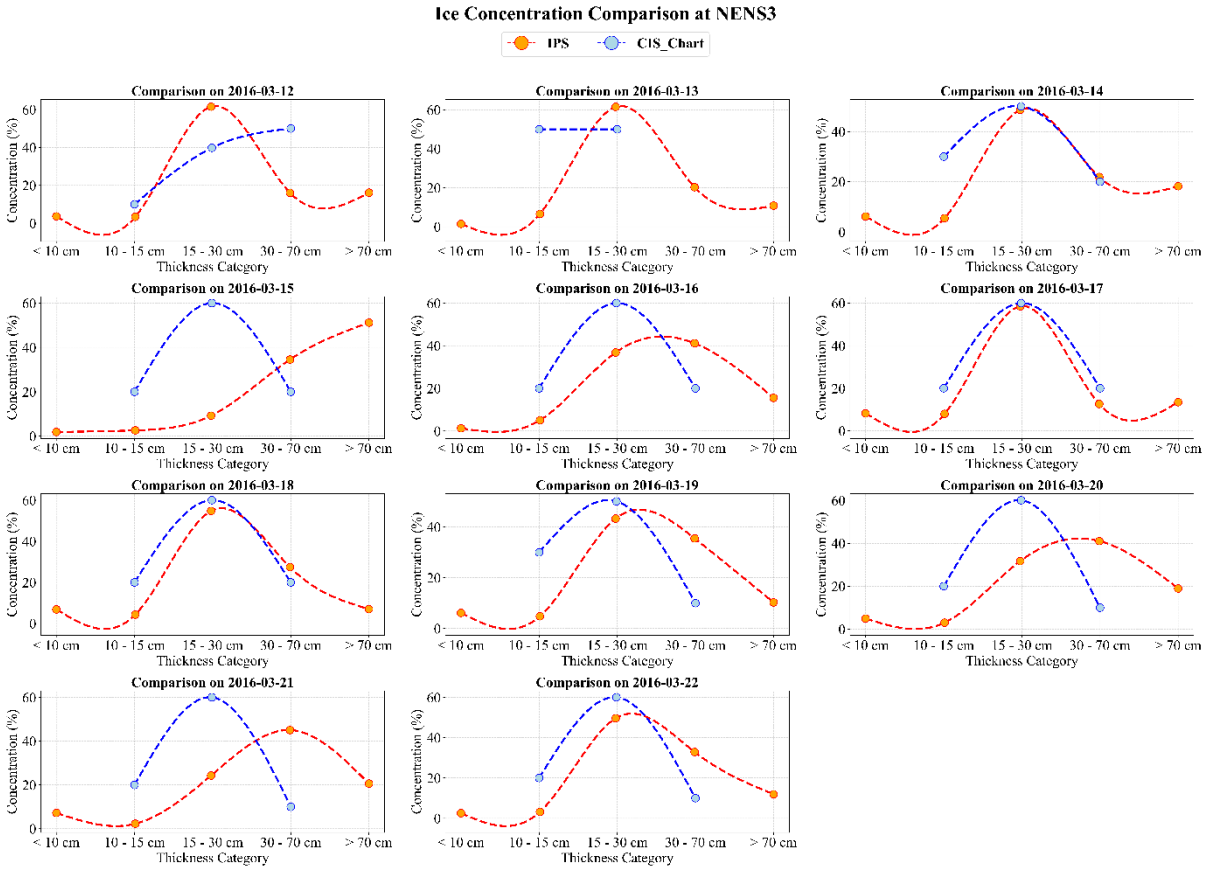

Figure 7: Comparison of Ice Concentration from IPS (yellow, green dashed line) and CIS-estimated (red, blue dashed line) at NENS3 (March 12–22, 2016).

CONCLUSIONS

This study presents a comparative assessment of sea ice thickness and concentration across the Northeast Newfoundland Shelf using high-resolution Ice Profiling Sonar (IPS) data and daily Canadian Ice Service (CIS) charts. Even after scaling the data spatially and temporally, significant differences remained.

For daily averages, IPS thickness at NENS1 ranged from 0.25 m to 1.17 m, while CIS values stayed between 0.12 m and 0.15 m. At NENS2, IPS varied from 0.27 m to 1.24 m, compared to CIS values between 0.12 m and 0.33 m. At NENS3, IPS ranged from 0.35 m to 0.85 m, while CIS stayed within 0.23 m to 0.35 m. These results show that IPS captures short-term and local variations more effectively than CIS, which presents a smoothed, regional picture. To improve spatial resolution, data interpolation was applied at four new locations (L1 to L4). At these points, IPS had a mean thickness of approximately 0.566 m and a standard deviation of 0.203 m, while CIS had a mean of 0.236 m and a standard deviation (SD) of 0.077 m. The larger variability in IPS indicates a better ability to detect localized thick ice events. For temporal resolution, IPS and CIS data were averaged every 2 hours. At NENS1, IPS had a mean of 0.316 m (SD-0.074 m) and CIS was 0.126 m (SD-0.004 m). At NENS2, IPS averaged 0.628 m (SD-0.376 m) and CIS 0.156 m (SD-0.023m). At NENS3, IPS averaged 0.367 m (SD-0.102 m) and CIS 0.317 m (SD-0.016 m), showing that IPS consistently recorded more detailed variations over time. In terms of concentration, IPS detected thicker ice categories (30–70 cm) but with lower frequency, while CIS consistently reported higher concentrations of thinner ice (10–30 cm), especially at NENS1 and NENS2.

These findings highlight the limitations of using ice charts alone for understanding dynamic ice conditions. High-resolution IPS data is essential for capturing localized and short-term changes in ice, which are critical for offshore operations, safety planning, and climate studies. Integrating multiple data sources improves the accuracy and reliability of sea ice monitoring.

ACKNOWLEDGEMENTS

We thank Equinor for providing funding for the deployment of the instrumentation used in this study. We also acknowledge the crew of the CCGS Amundsen for their support during the deployment and recovery operations. We thank ASL Environmental Sciences for carrying out the deployment and for their work in processing and analyzing the IPS and ADCP data. We gratefully acknowledge student funding support from Equinor and the Qanittaq Clean Arctic Shipping Initiative for portions of this research.

REFERENCES

Alexandrov, V., Sandven, S., Wahlin, J. and Johannessen, O.M., 2010. The relation between sea ice thickness and freeboard in the Arctic. *The Cryosphere*, 4(3), pp.373-380.

Mudge, T., Borg, K., Ersahin, K., Ross, E., Sadowy, D. and Barrette, J., 2016, October. Estimation and Validation of Floe Size Distribution from Upward Looking Sonars. In *OTC Arctic Technology Conference* (pp. OTC-27481). OTC.

King, J., Howell, S., Brady, M., Toose, P., Derksen, C., Haas, C. and Beckers, J., 2020. Local-scale variability of snow density on Arctic Sea ice. *The Cryosphere*, 14(12), pp.4323-4339.

Pustogvar, A. and Kulyakhtin, A., 2016. Sea ice density measurements. Methods and uncertainties. *Cold Regions Science and Technology*, 131, pp.46-52.

Timco, G.W. and Frederking, R.M.W., 1996. A review of sea ice density. *Cold regions science and technology*, 24(1), pp.1-6.

Warren, S.G., Rigor, I.G., Untersteiner, N., Radionov, V.F., Bryazgin, N.N., Aleksandrov, Y.I. and Colony, R., 1999. Snow depth on Arctic Sea ice. *Journal of Climate*, 12(6), pp.1814-1829.

Yulmetov, R., Thijssen, J., Shayanfar, H., Howell, M., and Paulin, M., 2022, June 'Pack ice characterization and its effect on ice loads offshore Newfoundland'. In: *Proceedings of the 26th IAHR International Symposium on Ice*. [Online] IAHR. Available at: https://www.iahr.org/library/technical?pid=474